Preferential Solvation of Phenol in Binary Solvent Mixtures. A Molecular Dynamics Study

Martin Dahlberg and Aatto Laaksonen*

Division of Physical Chemistry, Arrhenius Laboratory, Stockholm University, SE-106 91, Stockholm, Sweden

Received: November 8, 2005; In Final Form: December 4, 2005

Molecular dynamics computer simulations were carried out to study the preferential solvation of phenol in equimolar acetonitrile−water and ethanol−water binary mixtures. Two water models were used to investigate the model dependence of preferential solvation. The results are compared to recent intermolecular 1H NOESY experiments reported on the same systems. In the case of acetonitrile−water the local mole fraction obtained from simulations agrees quite well with experiments. In the case of ethanol−water there was a qualitative difference, which was observed for both water models. However, when comparing the degree of preferential solvation of the two cosolvents ethanol and acetonitrile with each of the two water models, the trend obtained from the simulations agrees with experimental data.

1. Introduction

Water is a unique solvent with a combination of superior solvation power for polar and ionic substances and a lack of it in the case of noble gas atoms and organic nonpolar substances. Because of its small size and high mobility, water molecules are able to access and cover surfaces of solute molecules to form a hydration shell. It is possible for water molecules to participate in many arrangements of hydrogen bonds due to its double donor and acceptor ability. Solvent mixtures of water and a water-miscible organic solvent are important media in many areas of industrial and environmental processes.[1,2] Mixed solvents may exhibit drastically different properties compared to their pure components. One well-known example is the water−dimethyl sulfoxide (DMSO) mixture which is commonly used as a cryosolvent due to its remarkably low freezing point (−70 °C for 3:1 water−DMSO mixture, while pure DMSO freezes already at +18.6 °C). Most importantly, binary mixtures may have very different solvation power than the neat liquids they are made of. For example, organic substances poorly soluble in water become completely dissolved in some aqueous liquid mixtures. On the molecular level this can be explained by a competition between the two molecular species in their interactions to the solute molecules. In a somewhat simplified picture, the nonpolar parts of the solvent molecules solvate nonpolar regions of the solute while the polar parts of the solvent molecules are more attracted to polar groups of the solute, for example by forming hydrogen bonds. This phenomenon is known as preferential solvation. Preferential solvation creates a complicated picture of competition and intermolecular interactions in delicate balance, leading to favorable synergy effects for solvation.

For atomic or molecular ions the preferential solvation in mixed liquids may sometimes become even selective.[3,4] Experimental evidence for selective solvation of ions in mixed solvents comes from electrochemical and spectroscopic studies.[5,6] The selective solvation phenomenon has received much attention, particularly after measurements by Strehlow and Koepp[7] in the late 1950s. Many theoretical attempts to explain selective solvation are found in the literature based on electrostatic, thermodynamic, and statistical mechanical arguments. Among the more technical applications, there are problems in hydrometallurgy of copper, silver, and gold, where preferential solvation is used to refine or regain precious metals from solutions of their salts. The reader is referred to excellent books and review articles concerning preferential and selective solvation.[1−6,8]

Various calorimetric approaches to study the preferential solvation of nonelectrolytes in mixed solvents are discussed by Korolev,[9] including cases where the composition dependence of enthalpy in binary mixtures is described by the Redlich−Kister equation.[10] An exact solution is found for the equation of the extended coordination preferential solvation model. An approach is suggested taking into account both preferential solvation and the effect of solvent reorganization in the solvation shell of the solute.

Computer simulation is an ideal method for the study of structure and dynamics of solutions, including mixed solvents on the molecular level. During the past two decades we have developed simulation schemes in order to combine molecular dynamics simulations and NMR relaxation measurements of liquids and solutions.[11] In particular, we have developed methods to calculate the intermolecular NMR relaxation times which are normally difficult to separate from the corresponding intramolecular relaxation contributions.[12] A method for calculating the relaxation matrix from the dipole−dipole correlation functions has previously been presented.[13] This procedure accounts for the dynamics of the dipole−dipole interaction and is an alternative to using r^{-6}-averaged distances. However, periodic boundaries used in molecular dynamics simulations impose an artificial correlation, which might make detailed calculation of NMR intermolecular relaxation parameters from molecular dynamics simulations difficult unless prohibitively large boxes are used.[14] Simulations of preferential solvation around tetraalkylammonium chlorides in acetonitrile−water mixtures have been reported and compared to mass spectrometry.[15]

In our early studies of water−acetonitrile mixtures[16] we observed so-called microheterogeneities among water molecules in low water concentration region. Water molecules were observed to form small chains: both linear and cyclic.[17] Later this was confirmed by Bertie and Lan[18] in their study of IR

* Corresponding author. E-mail: aatto@physc.su.se.

10.1021/jp056463e CCC: $33.50
Published on Web 01/21/2006

intensities on water−acetonitrile and by us[19] in detailed simulations on a much larger scale as well as in MD simulations by Mountain.[20] We have also studied preferential solvation of carbohydrates in water/DMSO and methanol/DMSO liquid mixtures simulations.[21−23] Simulations of preferential solvation of peptides in ethanol−water and TFE−water solutions have also been reported.[24] A convenient and powerful way to analyze and visualize the solvation structure is to use spatial distribution functions.[25]

Spectroscopic methods used to study preferential and selective solvation are mainly based on NMR, IR, and UV/vis spectral shifts. NMR is a powerful method for studying the local environment of molecules, with respect to both structure and dynamics. Nuclear dipole−dipole interactions play a major role in the NMR relaxation.[26] The cross-relaxation between solute and solvent nuclei can be used as a measure of the solvent environment around the solute, and due to the short-ranged nature of the dipole−dipole interaction only the local structure is probed. This effect is used in 2D 1H NOESY NMR spectroscopy, where the cross-peak intensity is related to the spin density around the solute.[27] Preferential solvation studies have lately become attractive due to the development of these techniques, and it is possible to study neutral molecules in solvent mixtures[28] as well as preferential solvation of specific sites around large molecules.[29,30] Since we are interested in modeling preferential solvation, a model for the intermolecular contribution to the relaxation rate under rapid tumbling conditions, $\mathbf{R}_1$, is useful:[31]

$$\mathbf{R}_1 \propto \tau_c \int_a^\infty r^2 [g(r)/r^6]\, dr \qquad (1)$$

where $g(r)$ is the radial distribution function of the solvent spins around the solute and a is the distance of closest approach between the nuclei. The correlation time, τ_c, reflects the rotation correlation time and the residence time of a solvent molecule in the first hydration sphere. This is a rather crude model, but it provides an interesting first look into preferential solvation via distance-weighted radial distribution functions and will work as a bridge between NMR-derived quantities and molecular dynamics simulations.

In this paper we wish to present our study of preferential solvation of the simple alcohol phenol in two mixed solvents: acetonitrile−water and ethanol−water. Phenol is readily soluble in many organic substances, for example in ethanol, but only sparsely soluble in water, 8 vol % at normal conditions. For modeling purposes phenol is attractive since it clearly has a hydrophobic and hydrophilic part. Also, the solvent mixtures have interesting properties due to their different hydrogen bond donor abilities and the liquid structure. Self-association has been observed in acetonitrile−water[32] and ethanol−water[33] and is important for the solvation of solutes dissolved in the mixtures.[30] A more complete description of preferential solvation would include also these effects. The aim in the present study is to examine the solvation structure of phenol. A thorough description of the mechanisms of clustering or self-assocation of the solvents is considered to be outside of the scope of this work.

This investigation is largely inspired by the recent work by Bagno where the solvation shell of organic molecules was probed by intermolecular 1H NOESY.[34] We anticipate that MD simulations and intermolecular NOE measurements would provide a powerful combination in studies of three-dimensional solvation structure and dynamics around macromolecules in solutions and in solvent mixtures in particular. In the next section we describe the simulation methods and the used molecular models in some detail. In section 3 we present and discuss our results while conclusions from this investigation are summarized in section 4.

TABLE 1: Solvents Simulated in This Work

system no.	solvent composition
I	504 SPC/E water
II	200 ethanol
III	200 acetonitrile
IV	128 ethanol + 128 SPC/E water
V	128 acetonitrile + 128 SPC/E water
VI	128 ethanol + 128 TIP3P water
VII	128 acetonitrile + 128 TIP3P water

2. Methods and Models

Five all-atom MD systems were prepared according to Table 1. For the systems IV−VII the mole fraction of water is $X_{H_2O} = 0.5$. We neglect the contribution to the mole fraction from the phenol, which is at a comparatively low concentration since a single phenol molecule was used in the simulations. We aimed to reproduce the low concentration used in experiments on the same system[28] and wanted to avoid possible solute−solute interactions in the simulation cell.

The OPLS force field[35,36] was used for the organic compounds phenol, acetonitrile, and ethanol. The models SPC/E[37] and TIP3P[38] were used for water. These two well-established water models were used to see force field dependences in the calculated quantities. The package GROMACS (3.2.1)[39,40] was used for preparation of the systems, simulation, and analysis unless otherwise stated. Simulations were run under NPT conditions with the Nosé-Hoover thermostat[41] (coupling time 0.2 ps) and the isotropic Parrinello-Rahman barostat[42] (coupling time 1 ps). Cubic periodic boundary conditions were used, and van der Waals potentials were cut off at 1 nm. Particle-mesh Ewald (PME) with a grid spacing of 0.1 nm was used to treat the electrostatic interactions. Systems were energy minimized prior to MD simulations, which were run with a time step of 2 fs with LINCS constraints on hydrogens.[43] Equilibration times of 500 ps were allowed for, during which densities and energies stabilized. The temperatures were thermostated to 300 K, and the external pressure was set to 1 bar. Production runs for the ternary systems were 40 ns long, and trajectories were saved every 0.2 ps. For the binary reference systems 19.5 ns trajectories were produced.

It is straightforward to investigate the isotropic preferential solvation through radial distribution functions (RDF), $g(r)$, and this was used as a starting point. Two approaches were used. First, RDFs were evaluated from different positions in the solute molecule to the center atom in the solvents. To assess the ratio of solvents, B and C, in a neighborhood of the center-of-mass of a group of atoms, which we call Q, the integrated RDFs were used, similar to a procedure described previously:[44]

$$n_{QB}(r') = \rho_B \int_0^{r'} g_{QB}(r) 4\pi r^2\, dr \qquad (2)$$

where ρ_B is the bulk number density of component B. The mole fraction of substance B at the distance r from compound Q, $x_B(r)$, was calculated from the expression

$$x_B(r) = \frac{n_{QB}(r)}{n_{QB}(r) + n_{QC}(r)} \qquad (3)$$

Second, RDFs from solute hydrogens to solvent hydrogens were evaluated. These distributions relate more closely to the NOE NMR experiment, where proton−proton cross relaxation is

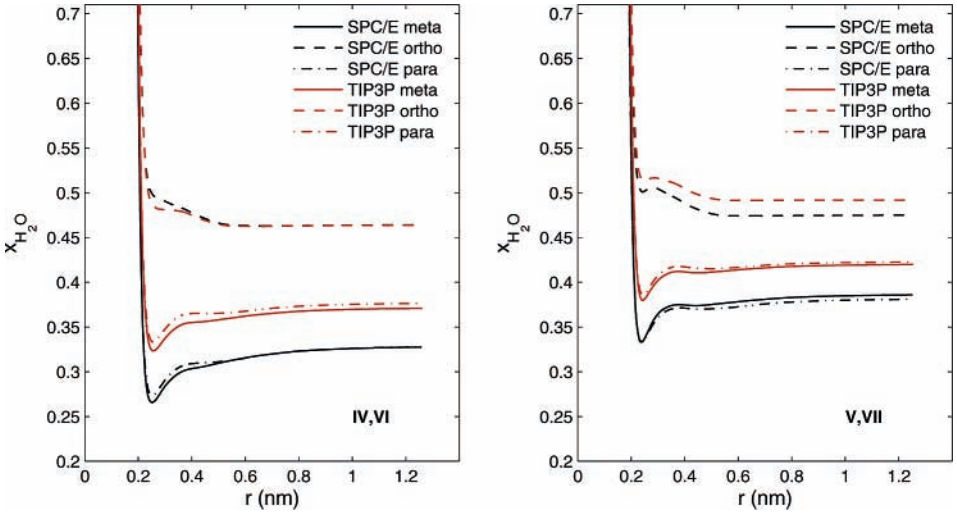

Figure 1. Local mole fraction of water around the ring hydrogens of phenol calculated from the r^{-6}-scaled RDFs (eq 4). Left: ethanol−water (simulations IV, VI). Right: acetonitrile−water (simulations V, VII).

measured. When several RDFs were obtained (e.g., the two types of nonpolar hydrogens in ethanol), the average value of their integrated RDF was used. An r^{-6}-weighted distribution was also calculated, in analogy with the association number, A_{ij}. The association number is in turn related to the Kirkwood−Buff number, G_{ij}, in for example the work of Holz et al.[45] The distance-dependent weighted distributions, $m(r')$, can be defined as

$$m_{QB}(r') = \rho_B \int_0^{r'} \frac{g_{QB}(r)}{r^6} 4\pi r^2 \, dr \qquad (4)$$

with a local mole fraction defined as in eq 3.

Spatial distribution functions[25] (SDF) were also calculated and visualized. The main advantage of the SDF in this analysis is the detailed geometric information about the solvation. A useful quantity in this context that illustrates the relative solvation is the *difference* spatial distribution function (ΔSDF) between two species in the solution:

$$g_{B-C}(x,y,z) = g_B(x,y,z) - g_C(x,y,z) \qquad (5)$$

where $g_B(x,y,z)$ is defined as the density of solvent B in the volume element surrounding the point x, y, z.[46] The SDFs were visualized done with VMD.[47] It should be noted that in principle the equilibrium spatial distribution functions could also be investigated by a Monte Carlo approach.

Diffusion coefficients were calculated from the mean-square deviations (MSD) of molecules. A linear function was fitted to the MSD from time 20 ps to 5 ns. The diffusion coefficients provide a good measure of the dynamics of the liquid mixture and can be determined experimentally very accurately. Diffusion is also a relevant property to investigate since many chemical processes rely on diffusion for mass transport. In the current investigation this information was mainly used as a validation of the force fields.

Although hydrogen bonding is a complex phenomenon which affects both the solvation thermodynamics and the dynamics, it is possible to give a functional definition of hydrogen bonding in the molecular dynamics trajectory based on geometric considerations. The hydrogen bonds in the present study were defined as the configurations with a donor−acceptor distance of no more than 0.35 nm and an angle between donor−hydrogen−acceptor of minimum 150°.

TABLE 2: Mole Fractions around Ring Hydrogens of Phenol from r^{-6}-Scaled RDFs[a]

	$x_{H_2O,SPC/E}$	$x_{H_2O,TIP3P}$
ethanol−water		
ortho	0.46	0.46
meta	0.33	0.37
para	0.33	0.38
acetonitrile−water		
ortho	0.48	0.49
meta	0.39	0.42
para	0.38	0.42

[a] The values were taken at a distance of 1.25 nm.

3. Results and Discussion

3.1. Radial and Spatial Distribution Functions. To be able to compare and identify our results with the experimental values of preferential solvation reported by Bagno et al.,[34] local mole fractions defined from the r^{-6}-scaled RDFs around the ring hydrogens are presented in Figure 1. The local mole fractions in the study by Bagno et al.[34] are reported as $x_{H_2O} = 0.4$ and $x_{H_2O} = 0.2$ in the acetonitrile−water and ethanol−water mixtures, respectively. The scaled RDF was chosen since it illustrates the r^{-6} dependence of the spin dipole−dipole interaction. This scaling separates the acetonitrile−water mixture from the ethanol−water mixture. Table 2 summarizes the mole fractions at the distance from the phenol hydrogen of 1.25 nm. For the *meta* and *para* positions the order of preferential solvation is clear with both water models, with the acetonitrile−water mixtures close to the experimental value at 0.4 (0.38−0.42) and the ethanol−water mixture between 0.33 and 0.38. At the *ortho* position the preferential solvation effect was smaller, mainly due to the high water content close to the hydroxyl group of the phenol. It is worth noting that the NOESY experiments performed at 2.3 T were unable to separate the peaks from the *ortho* and *para* protons of phenol. At distances over 0.6−0.7 nm the local mole fraction changes very little, reflecting the r^{-6} scaling.

The distance-weighted distributions indicate at least a qualitative agreement with experimental data. To establish the connection with the molecular description, the degree of preferential solvation was also calculated from the RDFs for the different sites of the phenol molecule. These data are presented in Figure 2. The local mole fraction of water around the hydroxyl group is higher than that measured from the center-of-mass. The local mole fraction of the cosolvent is analogously higher around the

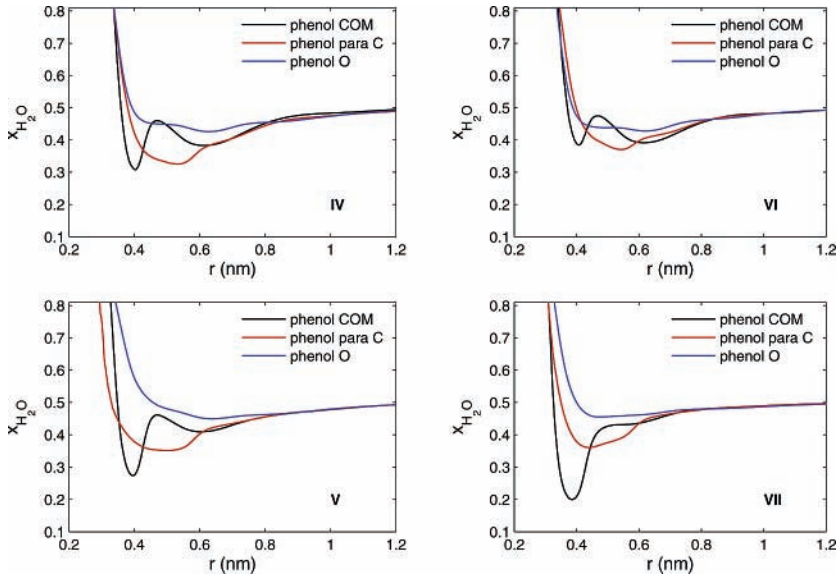

Figure 2. Local mole fraction of water as a function of distance from three different positions on phenol. Top left: ethanol−water mixture with SPC/E water (simulation IV). Top right: ethanol−water mixture with TIP3P water (simulation VI). Bottom left: acetonitrile−water mixture with SPC/E water (simulation V). Bottom right: acetonitrile−water mixture with TIP3P water (simulation VII). The three different positions are the center-of-mass (COM) of phenol (black), the *para* carbon (red), and the hydroxyl oxygen (blue).

para carbon. The relative ordering of preferential solvation in acetonitrile−water and ethanol−water mixtures is clear for the hydroxyl group, with ethanol being the more highly preferred solvent. For the other sites chosen it is notable that the same qualitative appearance is observed in both solvents but that acetonitrile has a high local mole fraction (0.7−0.8) at a distance of around 0.4 nm from the center-of-mass of phenol. Overall, the local mole fractions for the ethanol−water mixtures lie close together, whereas in the case of acetonitrile−water the mole fractions vary more with distance and appear quite different depending on which center of reference is used. The behavior of the local mole fraction at very small distances is explained by a small number of close approaches by the smallest molecule, i.e., water. This will give $x_{H_2O} \approx 1$ since the cosolvent cumulative number n_{QC} is very close to zero. The local mole fractions obtained from the unscaled RDFs also show that the *para* position has a similar behavior of preferential solvation in the 0.4−0.5 nm interval as the scaled RDFs do. This means that the preferential solvation described with the r^{-6}-scaled RDFs only accounts for the first solvation shell, and even so it does not include the strong association of acetonitrile to the center-of-mass, which lies close to the center of the phenol ring. The RDF is somewhat inadequate for describing the solvation structure around a nonspherical molecule, which motivates the use of the spatially resolved distribution function presented below.

In Figure 3 the ΔSDFs for the mixed solvent systems with the SPC/E water model are shown. The differences between the three sites show in Figure 2 confirm the picture from the spatial distribution functions, i.e., that positive (negative) densities are given where the oxygen of water (cosolvent) is in a higher local concentration. The localization of water around the hydroxyl group of phenol is clear, as is the smeared-out distribution of cosolvent around the ring. This illustrates the association of the cosolvent with the phenyl ring. Note the extension of the ethanol density surface, forming an ethanol-rich region compared to the corresponding position in the acetonitrile−water system. This behavior can also be observed in Figure 2, where the effect can be seen as fluctuations in the local mole fraction at distances above 0.6 nm. A notable difference between the ethanol−water and acetonitrile−water

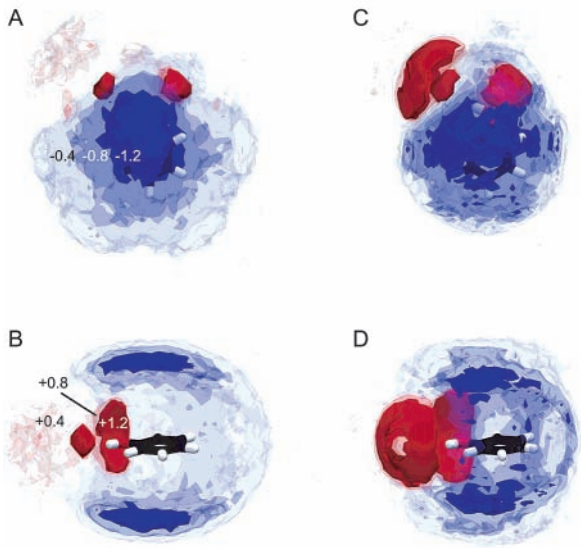

Figure 3. ΔSDF of solvents around phenol. Top (A and C) and side view (B and D). $g_{H_2O-ethanol}$ from simulation IV (A and B) and $g_{H_2O-acetonitrile}$ from simulation V (C and D). Red isodensities (+1.2, +0.8, +0.4) represent excess of water oxygen over cosolvent hydrogen acceptor (ethanol oxygen and acetonitrile nitrogen respectively). Blue isodensities (−1.2, −0.8, −0.4) represent excess of cosolvent hydrogen acceptor over water oxygen.

mixtures is the extent of the excess of water around the hydroxyl group. Ethanol competes more readily with water for the hydrogen bonds to phenol.

It is also notable that ethanol and acetonitrile form clusters in water at the simulated bulk mole fraction. The hydrogen bond structure of the ethanol−water mixture enables a fairly intimate mixture of the solvent molecules, but clear self-association between the species was shown. For the acetonitrile−water simulations regions rich in acetonitrile were observed, which were probably stabilized mainly by a strong dipole−dipole interaction. Water formed chains or small clusters. We do not go further into the mechanism for this homoclustering of the solvents but focus on the solute solvation. It should be noted that with the models used in the present study and at the

TABLE 3: Block Average of the Number of Hydrogen Bonds from Solvent to Phenol Hydroxyl Group

	av bond no.	
	SPC/E	TIP3P
water	2.191 ± 0.004	
ethanol	1.52 ± 0.01[a]	
acetonitrile	0.917 ± 0.002[a]	
water in acetonitrile−water	1.12 ± 0.05	1.11 ± 0.02
acetonitrile in acetonitrile−water	0.26 ± 0.02	0.27 ± 0.01
water in ethanol−water	1.04 ± 0.06	0.90 ± 0.06
ethanol in ehtanol−water	0.78 ± 0.05	0.87 ± 0.05

[a] No SPC/E water is present in the system.

TABLE 4: Self-diffusion Coefficients [10^{-5} cm^2 s^{-1}] for Components of Simulated Systems

	SPC/E	TIP3P	expt
water	2.58 ± 0.02		2.3[a]
ethanol	1.38 ± 0.04		1.24[b]
acetonitrile	4.87 ± 0.13		4.3[a]
water in acetonitrile−water	1.89 ± 0.05	3.33 ± 0.16	3.0[a]
acetonitrile in acetonitrile−water	2.28 ± 0.02	3.41 ± 0.22	3.3[a]
water in ethanol−water	1.03 ± 0.03	1.99 ± 0.10	0.875[c]
ethanol in ethanol−water	0.90 ± 0.01	1.34 ± 0.23	0.72[d]

[a] From ref 19. [b] From ref 48. [c] From ref 49. [d] Interpolated from ref 50.

equimolar mixture the radial structure of the solvent−solvent distributions was similar in the case of ethanol−water and acetonitrile−water.

3.2. Hydrogen Bonding of Phenol. In contrast to the aromatic ring, where solvation is due to hydrophobic interactions, the hydroxyl group readily forms hydrogen bonds to the solvent donors and acceptors. Block-averaged data on the number of bonds from the solvent to phenol hydroxyl are presented in Table 3. Water and ethanol act as both donors and acceptors, which is reflected in their high average number of hydrogen bonds. Acetonitrile participates as a hydrogen bond acceptor, and in the pure acetonitrile system this bond is present at about 90% of the simulated time. In the acetonitrile−water mixture the amount of hydrogen bonding between acetonitrile and phenol is reduced to roughly 30%. The SPC/E and TIP3P models give similar results in the acetonitrile−water mixtures. For the ethanol−water mixture the ratio of hydrogen bonding from ethanol and water is 1.33 in the case of SPC/E and 1.03 in the case of TIP3P.

3.3. Dynamical Properties of the Simulated Liquid Mixtures. Diffusion is a sensitive probe of the dynamics in the liquid on the molecular length scale. Diffusion coefficients were calculated for the solvent species, and these are summarized in Table 4. The overall agreement with experimental data was reasonable, with some differences between the two water models. The underestimation of the diffusion coefficient in acetonitrile−water mixtures with the SPC/E water model has been observed in simulation before.[19] The explanation given there is reasonable: that the effective charges on the water molecules are large due to taking the overall polarization into account and that this gives an overly structured liquid. The situation is reversed for the ethanol−water mixture, where the SPC/E model gives more reasonable values of the diffusion coefficient, and TIP3P overestimates diffusion. It is well-established that TIP3P models water with a too high diffusion coefficient, and here we see the effect carrying over to the cosolvent ethanol. Since the atomic charges are optimized for the pure liquids, it is possible that mixtures do not reproduce experimental data as accurately as desirable. For static properties such as spatial distribution around the solute, this is probably of little importance. However, any inaccurately modeled dynamics might be significant for comparisons with NMR-related quantities, where intermolecular time correlation functions are important. The limiting factor for comparison with NMR experiments in our view is the periodic boundary conditions which introduce artificial contributions to the dipole−dipole correlation function with the box sized used in the present study. The values for the diffusion obtained in this work show however that the models used give a reasonable behavior with respect to dynamics.

4. Conclusions

From the detailed molecular information in molecular dynamics simulations the solvation structure and preference of phenol have been investigated. Different measures of the degree of preferential solvation have been used for equimolar mixtures of ethanol−water and acetonitrile−water. Local mole fractions around different sites at the phenol molecule showed that the solvation is preferential and that there is a qualitative agreement with NMR experiments. To relate the simulated quantities to the NMR experiment, the distance dependence of the spin dipole−dipole interaction was taken into account through the use of a distance-weighted distribution function. The two water models gave slightly different quantitative results but overall showed the robustness of the simulations. It should also be noted that the experimental results used to assess the validity of our results[34] are semiquantitative in the sense that several approximations are made in the treatment of the NMR data. In the ethanol−water models we were unable to show the strong preferential solvation reported experimentally.[34] It is possible that a reparametrization of the force field would be needed to approach the experimental values. However, since it is not clear exactly how the quantities determined in our simulations and in the experiments should be related to each other, it is not clear that general improvements to the force field would be accomplished by matching the local mole fractions.

In the simulations, the dynamic dependence of the dipole−dipole interaction which is important in spin relaxation is not taken into consideration in the present study, since evaluation of this property is difficult with reasonable box sizes.[14] Diffusion is one of the dynamical properties that influences NOE transfer, and since diffusion data from the present study show deviations from experimentally determined diffusion data in at least one of the mixed systems, we chose not to investigate the dynamics of the solutions more closely.

Ethanol participates as both hydrogen donor and acceptor in bonding to phenol. Acetonitrile acts as an acceptor and competes with water. The structure of the acetonitrile−water mixture decreases the amount of hydrogen bonding to phenol compared to the expected degree of solvation from the pure solvents.

Acknowledgment. This work has been supported by the Swedish Research Council (VR) and Carl Trygger Foundation. Generous allocation of computing time by SNIC is gratefully acknowledged. The authors thank Dr. Dallas Warren for providing a modified version of the g_sdf tool for calculating SDF's and Prof. Arnold Maliniak for critical reading of the manuscript.

References and Notes

(1) Reichardt, C. *Solvents and Solvent Effects in Organic Chemistry*, 2nd ed.; VCH Verlag: Weinheim, 1988.

(2) Marcus, Y. *Solvent Mixtures. Properties and Selective Solvation*; Marcel Dekker: New York, 2002.

(3) Janardhanan, S.; Kalidas, C. *Rev. Inorg. Chem.* **1984**, *6*, 101−148.
(4) Kessler, Y. M.; Vaisman, I. I.; Kiselev, M. G.; Puhovski, Y. P. *Acta Chim. Hung.* **1992**, *129*, 787−824.
(5) Schneider, H. *Solute−Solvent Interaction*; Marcel Dekker: New York, 1969; Chapter 5, pp 301−343.
(6) Schneider, H. *Solute−Solvent Interaction*; Marcel Dekker: New York, 1976; Chapter 5, pp 103−148.
(7) Strehlow, H.; Koepp, H.-M. *Z. Elektrochem.* **1957**, *62*, 327−344.
(8) Strehlow, H.; Schneider, H. *Pure Appl. Chem.* **1971**, *25*, 327−344.
(9) Korolev, V. P. *Russ. J. Gen. Chem.* **2000**, *70*, 1859−1866.
(10) Redlich, O.; Kister, A. T. *Ind. Eng. Chem.* **1948**, *40*, 341−345.
(11) Odelius, M.; Laaksonen, A. *Theoretical and Computational Chemistry: Molecular Dynamics−From Classical to Quantum Methods*; Elsevier: Amsterdam, 1999; Chapter 8, pp 281−324.
(12) Odelius, M.; Laaksonen, A.; Levitt, M. H.; Kowalewski, J. *J. Magn. Reson. A* **1993**, *105*, 289−296.
(13) Peter, C.; Daura, X.; v. Gunsteren, W. F. *J. Biomol. NMR* **2001**, *20*, 297−310.
(14) Grivet, J.-P. *J. Chem. Phys.* **2005**, *123*, 034503.
(15) Saielli, G.; Scorrano, G.; Bagno, A.; Wakisaka, A. *ChemPhysChem* **2005**, *6*, 1307−1315.
(16) Kovacs, H.; Laaksonen, A.; Kowalewski, J. *J. Phys. Chem.* **1990**, *94*, 7378−7385.
(17) Kovacs, H.; Laaksonen, A. *J. Am. Chem. Soc.* **1991**, *113*, 5596−5605.
(18) Bertie, J. E.; Lan, Z. *J. Phys. Chem. B* **1997**, *101*, 4111−4119.
(19) Bergman, D.; Laaksonen, A. *Phys. Rev. E* **1998**, *58*, 4706−4715.
(20) Mountain, R. D. *J. Phys. Chem. A* **1999**, *103*, 10744−10748.
(21) Vishnyakov, A.; Widmalm, G.; Laaksonen, A. *Angew. Chem., Int. Ed.* **2000**, *39*, 11207−11215.
(22) Vishnyakov, A.; Laaksonen, A.; Widmalm, G. *J. Mol. Mod. Graph.* **2001**, *19*, 338−342.
(23) Vishnyakov, A.; Lyubartsev, A. P.; Laaksonen, A. *J. Phys. Chem. A* **2001**, *105*, 1702−1710.
(24) Fioroni, M.; Diaz, M. D.; Burger, K.; Berger, S. *J. Am. Chem. Soc.* **2002**, *124*, 7737−7744.
(25) Kusalik, P. G.; Laaksonen, A.; Svishchev, I. M. *Theoretical and Computational Chemistry: Molecular Dynamics−From Classical to Quantum Methods*; Elsevier: Amsterdam, 1999; Chapter 3, pp 61−98.
(26) Bryant, R. G. *Annu. Rev. Phys. Chem.* **1978**, *29*, 167−88.
(27) Macura, S.; Ernst, R. *Mol. Phys.* **1980**, *41*, 95−117.
(28) Bagno, A.; Scorrano, G.; Tiz, S. *J. Am. Chem. Soc.* **1997**, *119*, 2299−3000.
(29) Bagno, A.; Rastrelli, F.; Scorrano, G. *J. Magn. Reson.* **2004**, *167*, 31−35.
(30) Rastrelli, F.; Saielli, G.; Bagno, A.; Wakisaka, A. *J. Phys. Chem. B* **2004**, *108*, 3479−3487.
(31) Langer, H.; Hertz, H. G. *Ber. Bunsen-Ges. Phys. Chem.* **1977**, *81*, 478−90.
(32) Spångberg, D. Cation solvation in water and acetonitrile from theoretical calculations. Ph.D. Thesis, Uppsala University, Sweden, 2003.
(33) Wakisaka, A.; Ohki, T. *Faraday Discuss.* **2005**, *129*, 231−245.
(34) Bagno, A. *J. Phys. Org. Chem.* **2002**, *15*, 790−795.
(35) Jorgensen, W. L.; Maxwell, D. S.; Tirado-Rives, J. *J. Am. Chem. Soc.* **1996**, *118*, 11225−11236.
(36) Price, M. L. P.; Ostrovsky, D.; Jorgensen, W. L. *J. Comput. Chem.* **2001**, *22*, 1340−1352.
(37) Berendsen, H. J. C.; Grigera, J. R.; Straatsma, T. P. *J. Phys. Chem.* **1987**, *91*, 6269−6271.
(38) Jorgensen, W. L.; Chandrasekhar, J.; Madura, J. D.; Impey, R. W.; Klein, M. L. *J. Chem. Phys.* **1983**, *79*, 926.
(39) Berendsen, H. J. C.; Van Der Spoel, D.; Van Drunen, R. *Comput. Phys. Commun.* **1995**, *91*, 43−56.
(40) Lindahl, E.; Hess, B.; van der Spoel, D. *J. Mol. Mod.* **2001**, *7*, 306−317.
(41) Hoover, W. *Phys. Rev. A* **1985**, *31*, 1695−1697.
(42) Parrinello, M.; Rahman, A. *J. Appl. Phys.* **1981**, *52*, 7182−7190.
(43) Hess, B.; Bekker, H.; Berendsen, H. J. C.; Fraaije, J. G. E. M. *J. Comput. Chem.* **1997**, *18*, 1463−1472.
(44) Ben-Naim, A. *Pure Appl. Chem.* **1990**, *62*, 25−34.
(45) Holz, M.; Grunder, R.; Sacco, A.; Meleleo, A. *J. Chem. Soc., Faraday Trans.* **1993**, *89*, 1215−1222.
(46) g-sdf tool for Gromacs. An updated version obtained as a personal communication from D. Warren.
(47) Humphrey, W.; Dalke, A.; Schulten, K. *J. Mol. Graphics* **1996**, *14*, 33−38.
(48) Wensink, E. J. W.; Hoffmann, A. C.; van Maaren, P. J.; van der Spoel, D. *J. Chem. Phys.* **2003**, *119*, 7308−7317.
(49) Price, W. S.; Ide, H.; Arata, Y. *J. Phys. Chem. A* **2003**, *107*, 4784−4789.
(50) Harris, K. R.; Newitt, P. J.; Derlacki, Z. J. *J. Chem. Soc., Faraday Trans.* **1998**, *94*, 1963−1970.